Traffic jams and hysteresis in driven one-dimensional systems

O. M. Braun,[1,2] B. Hu,[1,3] A. Filippov,[1,4] and A. Zeltser[1,4]
[1]*Department of Physics and CNS, HK Baptist University, Hong Kong, China*
[2]*Institute of Physics, National Ukrainian Academy of Sciences, UA-252022 Kiev, Ukraine*
[3]*Department of Physics, University of Houston, Houston, Texas 77204*
[4]*Physical-Technical Institute, National Ukrainian Academy of Sciences, UA-340114 Donetsk, Ukraine*
(Received 12 January 1998)

The driven underdamped chain of anharmonically interacting atoms in the sinusoidal external potential is studied. It is shown that due to the interatomic interaction the system exhibits hysteresis for any nonzero rate of changing of the dc driving force. Before the transition to the running state the system passes through the traffic-jam inhomogeneous state. The system behavior is explained with the help of two simple models, the discrete lattice-gas model with two states of atoms, and the continuum mean-field model based on the Fokker-Planck equation. [S1063-651X(98)10507-X]

PACS number(s): 05.40.+j, 05.70.Ln, 46.10.+z, 82.20.Mj

I. INTRODUCTION

Driven diffusive systems belong to the simplest models of nonequilibrium statistical mechanics. These systems are characterized by a locally conserved density, with a uniform external field setting up a steady mass current. The systems of this class have wide application in modeling of charge and mass transport in solids. Recently the driven diffusive models have been used in tribology, where the driving force emerges due to motion of one of two substrates, which are separated by a thin atomic layer.

In the context of tribology, the generalized Frenkel-Kontorova (FK) model has been studied [1–6]. In this model, a one- or two-dimensional atomic system is placed into the external periodic potential, and the atomic current j in response to the dc driving force F is studied by numerical solutions of Langevin motion equations. The simulations showed that the function $j(F)$ exhibits hysteresis: when the force increases, the system goes from the low-mobility regime to the high-mobility state, where all atoms move with almost maximum velocity. But if the dc force is then decreased, the high-mobility state survives to quite small values of F, and then jumps abruptly to the low-mobility state. In addition, during the transition the atoms have a tendency to be organized in compact groups of two different types, one consisting only of slowly moving atoms (which resemble ''traffic jams''), and another of ''running'' atoms moving with the maximum velocity. To explain these issues, let us first describe the model under consideration in more detail.

Model. We consider a chain of N atoms subjected to the sinusoidal external potential with the amplitude $E_0=2$ and the period $a=2\pi$, the atomic mass is $m=1$ (this defines our system of units). The equation of motion for the atomic coordinate x_i is the following:

$$\ddot{x}_i+\eta\dot{x}_i+\sin x_i+\frac{\partial}{\partial x_i}[V(x_{i+1}-x_i)+V(x_i-x_{i-1})] = F+\delta F_i(t), \tag{1}$$

where $1\leqslant i\leqslant N$, and periodic boundary conditions are assumed. The substrate potential has M wells on the chain length, so that the dimensionless atomic concentration is $\theta=N/M$, and the average distance between the atoms is $a_A=a/\theta$. In simulation we used the value $\theta=2/3$ everywhere. The coefficient η corresponds to the external viscous damping due to energy exchange between the chain and the substrate. For the interaction of nearest-neighboring atoms we took the Toda (exponential) potential

$$V(x)=V_0e^{-\beta x}, \tag{2}$$

so that the characteristic radius of interaction is $r=\beta^{-1}$. The dimensionless elastic constant, which is the main parameter of the classical FK model, is defined as $g=a^2V''(a_A)/2\pi^2E_0$ (e.g., see Ref. [7]). For the potential (2), g is equal to

$$g=V_0\beta^2\exp(-\beta a_A). \tag{3}$$

To all atoms we applied a dc force F and also the Gaussian random force $\delta F_i(t)$, $\langle\delta F_i(t)\delta F_j(t')\rangle=2\eta T\delta_{ij}\delta(t-t')$, which models a thermal bath with temperature T. In the simulation we calculated the average system velocity and then the mobility B defined as

$$B=\langle\langle v\rangle\rangle/F, \tag{4}$$

where $\langle\langle\cdots\rangle\rangle$ stands for the averaging over the system and also the averaging over time. If the substrate potential is absent, for any $F>0$ after a time $t\sim\eta^{-1}$ the system reaches a steady state characterized by the maximum mobility $B_f=\eta^{-1}$. In addition, we calculated the velocity correlation function

$$K_l=\langle\langle(\dot{x}_{i+l}-\dot{x}_i)^2\rangle\rangle, \tag{5}$$

which will be used to distinguish a homogeneous steady state from inhomogeneous ones.

Hysteresis. Typical hysteretic dependences $B(F)$ are presented in Figs. 1 and 2 for the harmonic and exponential interactions, correspondingly. These dependences were cal-

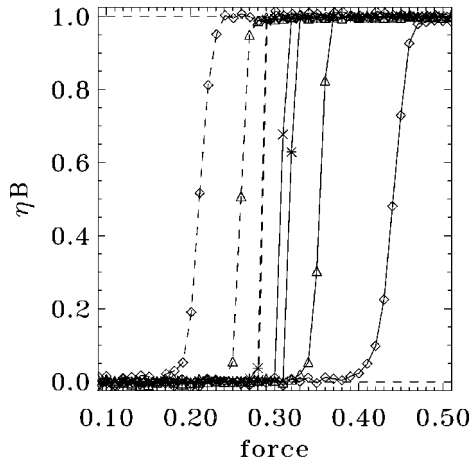

FIG. 1. Hysteresis $B(F)/B_f$ for the standard Frenkel-Kontorova model. Solid curves correspond to increasing force and dashed curves to decreasing force processes. The four curves are for four rates of force changing $R=\Delta F/3i_R\tau_0$, where $\Delta F=0.01$, $\tau_0=2\pi$ is the characteristic period of the system, and the value of i_R is indicated by different symbols: diamonds for $i_R=1$, triangles for $i_R=10$, asterisks for $i_R=10^2$, and crosses for $i_R=10^3$. The model parameters are $\theta=2/3$, $N=256$, $g=0.1$, $T=0.1$, and $\eta=0.1$.

culated with the algorithm described in detail in Ref. [4]. Namely, we slowly changed the force with small steps, the force was changed on the value $\Delta F=0.01$ during the time τ_R, then we waited the time τ_R to allow the system to equilibrate, and after that we measured the velocity and correlations during the time τ_R, thus the average rate of force changing is $R=\Delta F/3\tau_R$. Four curves in Figs. 1 or 2 were calculated for four rates of F changing, which differ by ten times one from the next one. As seen, a width of the hysteretic loop decreases with decreasing of R, but a well defined hysteresis still exists even for the smallest rate $R=5.3\times10^{-7}$. Thus, the simulation prompts that the hysteresis could survive for any rate of force changing. As will be shown in the present paper, the hysteretic behavior should exist for any nonzero rate R. Taking into account the one dimensionality of the FK model, the existence of hysteresis at $T>0$ is not trivial.

Traffic-jam state. Comparing the hysteretic curves of Fig. 1 for the standard FK model with those of Fig. 2 calculated

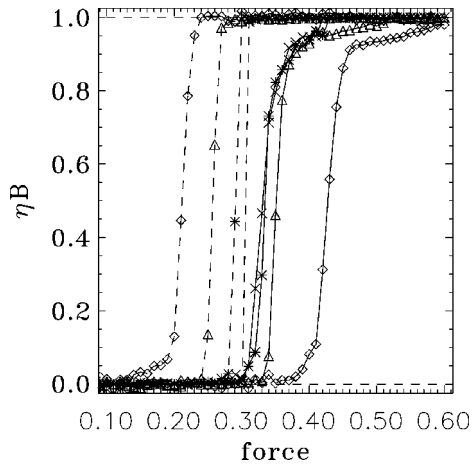

FIG. 2. The same as in Fig. 1 but for exponential interatomic interaction (2) with $\beta=1/\pi$.

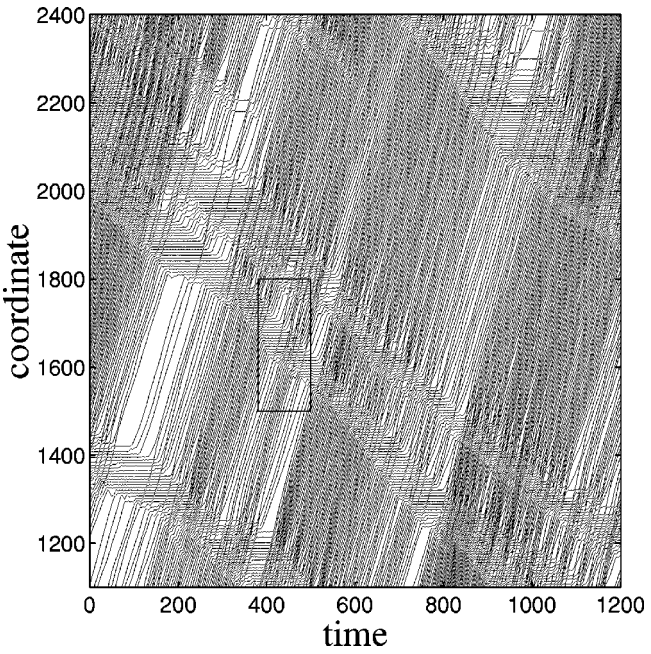

FIG. 3. Atomic trajectories for the exponential interaction with $\beta=1/\pi$ at the fixed force $F=0.33$. Other parameters are the same as in Fig. 1. The rectangle is shown enlarged in Fig. 4.

for the anharmonic (exponential) interaction, one can see the following essential differences between them. For the harmonic interaction, the system goes directly from the low-mobility (''locked'') state to the high-mobility (''running'') state. Although the system may be found in steady states with intermediate values of B, e.g., $B/B_f\sim0.5$, these states, as we checked by analyzing the atomic trajectories, always correspond to a *homogeneous* state on a spacial scale larger than the lattice constant a. On the other hand, for anharmonic interaction between the atoms, the system passes through intermediate states which are *spacially inhomogeneous*. In this type of steady states, the system splits into two qualitatively different regions, which differ by atomic concentration and velocities. A typical picture of atomic trajectories is presented in Fig. 3. One can clearly distinguish ''running'' regions, where atoms move with almost maximum velocities, and ''traffic-jam'' regions, where atoms are almost immobile. The regions characterized by a larger atomic concentration and smaller (almost zero) atomic velocities are called ''jams'' in what follows. In Fig. 4, which shows a small portion extracted from Fig. 3, one can see the dynamics of a single jam. The jam grows from its left-hand side due to incoming atoms which stop after collisions with the jam and then join to the jam. From the right-hand side, the jam shortens, emitting atoms to the right-hand-side running region. In addition, in Fig. 4 one can also see a detailed scenario of the jam's dynamics: when an incoming atom collides with the jam, it creates a kink (local compression) in the jam. This kink then runs to the right-hand side of the jam and stimulates there the emission of the atom into the right-hand-side running domain. Thus, simulations show that the traffic-jam state may correspond to a steady state of the system. In the present work we show that this state is the stable steady state, and find the conditions under which the traffic-jam state should emerge.

Thus, in the present paper we concentrate on the follow-

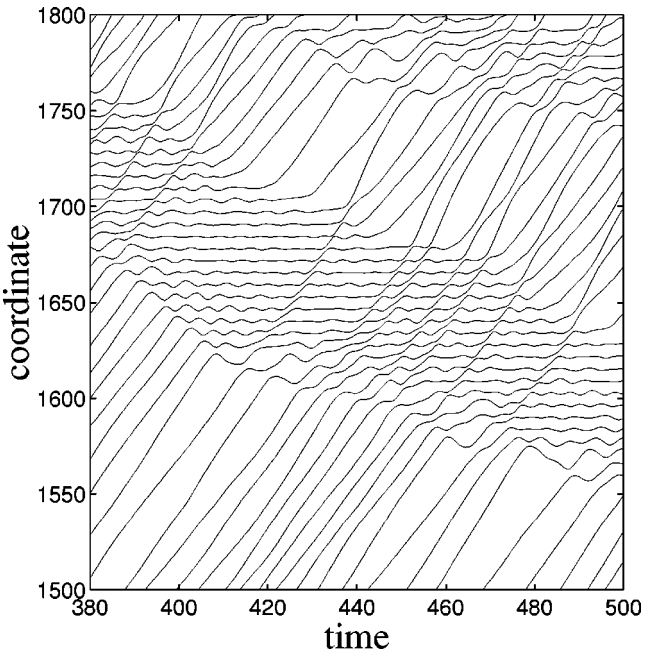

FIG. 4. A single jam of Fig. 3.

ing two questions. Does the hysteresis really exist in a one-dimensional system? Does the state with jams correspond to a stable steady state?

The paper is organized as follows. First, in Sec. II we show that a system state with jams corresponds to a strange attractor and, therefore, it should be dynamically stable. Then, in Sec. III we investigate conditions under which the system state with jams should emerge, and show that an anharmonicity of the interatomic interaction is the necessary condition for the transition to the traffic-jam state. Both these sections are based on computer simulation. In the next two sections we introduce two simple models which allow an analytical description of the phenomena under investigation. Namely, in Sec. IV we develop and study a simple *discrete* lattice-gas model. This model is characterized by two states of atoms, the ''immobile'' state which is the same as in the standard lattice-gas model, and the ''running'' state where the atoms jump in one direction only. The model exhibits the existence of traffic jams, a nonlinear dependence of mobility on the jump probability, and, moreover, it already shows the hysteresis. In Sec. V we reduce the set of Langevin equations (1) to a single mean-field *continuous* Fokker-Planck equation, which then is used to explain qualitatively the existence of hysteretic behavior in the FK model. Finally, Sec. VI concludes the paper with a summary of the results and a discussion of the general aspects of the traffic-jam behavior.

II. ATTRACTOR

The first question we are interested in is the following. Is the inhomogeneous state with traffic jams really a stable steady state of the system? This question can be reformulated as the following two questions. (1) Is the corresponding configuration in the phase space an attracting one? (2) If it is attracting, what is an attractive domain for the state with traffic jams? In turn, this question is coupled directly with one of a possible choice of initial conditions leading to the inhomogeneous state. Also, the same question can be reformulated as one about the stability of the traffic-jam state at nonzero temperatures.

First, let us recall some facts known from studies of a more simple problem of Brownian motion of a single atom (or a system of noninteracting atoms) in a periodic potential, which has been studied widely (e.g., see Ref. [8]). In this case Eqs. (1) reduce to the set of equations for N independent atoms

$$\ddot{x}_i + \eta \dot{x}_i + \sin x_i = F + \delta F_i(t). \tag{6}$$

Without the noise terms $\delta F_i(t)$ every equation from this set becomes a deterministic one which reads simply

$$\ddot{x} + \eta \dot{x} + \sin x = F. \tag{7}$$

Equation (7) can easily be solved for any initial conditions. The corresponding phase pattern on the (x,v) plane is shown in Fig. 5(a).

As is well known, for a Hamiltonian system different phase trajectories cannot intersect each other except the ones going through singular (fixed) points (the singular point is defined as a point where both $\dot{x} \equiv v$ and $\ddot{x} \equiv dv/dt$ vanish). At large forces, $F > F_f \equiv \pi E_0/a$, Eq. (7) has no singular points at all. The total potential $U_{\text{eff}}(x) = 1 - \cos x - xF$ has no minima at $F > F_f$, and Eq. (7) has ''running'' solutions only. On the other hand, at smaller forces, $F < F_f$, Eq. (7) has two kinds of singular points. The first one corresponds to the

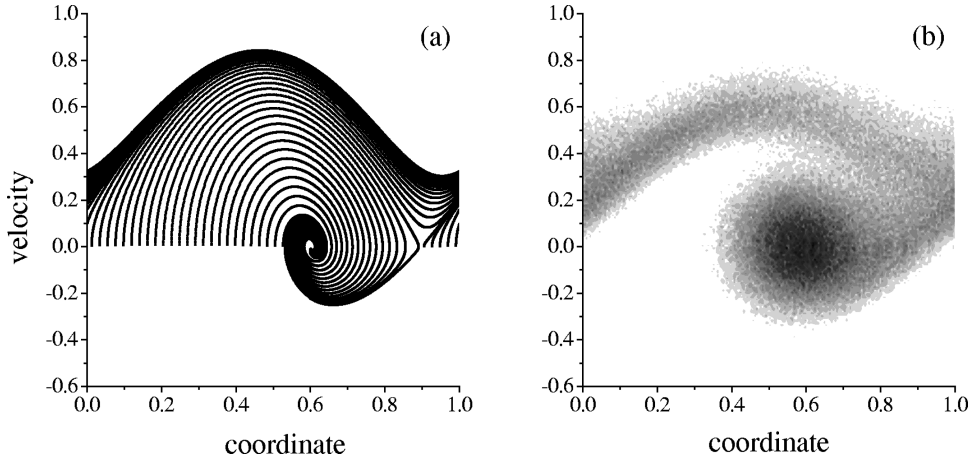

FIG. 5. Phase pattern for a single atom in periodic potential. (a) Flow lines for the deterministic equation (7) at $\eta = 0.5$, $F = 0.3$. Only the trajectories within one period of the substrate potential (normalized to 1) started from the line $\dot{x} = 0$ are shown. (b) Phase pattern for Eq. (6) with random noise corresponding to nonzero temperature $T = 0.1$. The grey scale map presents the distribution function $W(x,\dot{x};t)$ for the steady state at $t \to \infty$.

trivial static solution which describes the atom locked at a minimum of $U_{\rm eff}(x)$, e.g., at the position $x=\sin^{-1} F$, $\dot{x}=0$. This fixed point is the stable (focal) one, and the trajectories approaching it are spiral in the underdamped case. The second singular point is the unstable (saddle) one. It corresponds to the atom at a maximum of the total potential $U_{\rm eff}(x)$. At small dc forces, $F<\min(F_b,F_f)$, where $F_b \simeq (4/\pi)\eta\sqrt{mE_0}$, almost every solution of Eq. (7) is finished in the focal point when $t\to\infty$. In the overdamped case, $\eta > \eta_c$, where $\eta_c \simeq \pi^2\sqrt{E_0}/4a\sqrt{m}\approx 0.56$, Eq. (7) at $t\to\infty$ has either the locked solution (if $F<F_f$) or the running one (if $F>F_f$). But in the *underdamped* case, $\eta<\eta_c$, there is the interval of forces $F_b<F<F_f$, where Eq. (7) admits both types of solutions, the locked solution and the running one, simultaneously. In this case there is a special trajectory called the separatrix, which passes through the saddle points and separates the spiral trajectories attracting to the focus from the trajectories which go to the running solution. Depending on the initial state, the evolution of the system ends up in one of two attracting configurations: the trajectories below the separatrix are attracted to the trivial fixed point and finish in the locked state, while the other ones go to an attracting curve which corresponds to the running state.

The existence of two attracting domains leads to bistability of motion of the Brownian particle in the periodic potential without noise. However, the situation is changed drastically when one turns on a noise: any small but nonzero temperature makes it possible for the trajectory to jump from one side of the separatrix to the other. Figure 5(b) shows the transformation of the phase pattern of Fig. 5(a) in the presence of a small noise. Instead of trajectories, we plot in Fig. 5(b) the gray-scale map for the distribution function $W(x,\dot{x};t)$ at $t\to\infty$ (the method of its calculation is described below in this section). As seen from Fig. 5(b), the regions near the $T=0$ attracting trajectories are covered quite densely by randomly perturbed trajectories. However, one could see (and also it can be directly tested for every flow line separately) that the trajectories can ''jump'' across the separatrix in the vicinity of the saddle points. These jumps show that fluctuations can push the atoms out of the locked state as well as fix them back from the running state. Namely, these jumps completely destroy the bistability (and, therefore, the hysteresis) for the system of noninteracting atoms at nonzero temperatures [8].

Let us return now to the system of *interacting* atoms. In the state with traffic jams every atom can be found in both the running state and the locked state at different time moments. This means that the projection of the atomic trajectory onto the plane (x,v) should exhibit transitions from a vicinity of the locked state to the running one and vice versa. Indeed, the respective $2N$-dimensional phase pattern shows some regular channels which connect the running and locked states of the same atom. To depict these channels explicitly and to compare the results with those for the case of noninteracting atoms, we plot together in one Fig. 6 the (x,v) projections of the trajectories of all atoms at $T=0$. A direct comparison of this figure with the analogous pattern of Fig. 5(a) for the case of noninteracting atoms (both patterns are for $T=0$) shows that the interatomic interaction leads to the following new effects.

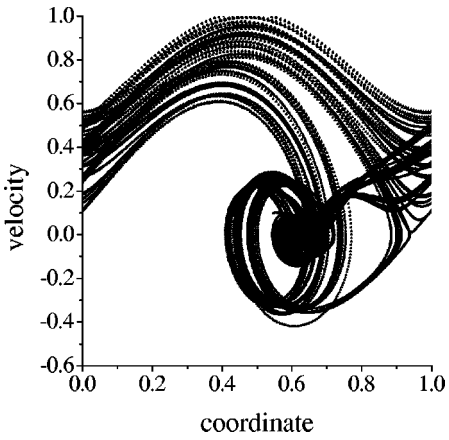

FIG. 6. Typical flow lines of the $T=0$ strange attractor for the system of interacting atoms calculated for the following system parameters: $\theta=2/3$, $g=0.1$, $\beta=1/\pi$, $\eta=0.5$, and $F=0.3$.

(1) The atoms can visit both the locked and running attracting regions.

(2) These regions are connected by two specific channels. Along these channels the atoms cross the separatrix [defined above for Eq. (7)] in the vicinity of the saddle points even without the temperature driven jumps.

(3) When one starts with different random initial configurations, the system reaches the typical trajectories in phase space ''stably.'' Therefore, the configuration of flow lines presented in Fig. 6 is an *attractor* of the system under consideration, at least within the accuracy of the simulation.

(4) Even at $T=0$ this attractor is *chaotic*.

The last statement needs an additional comment. From Fig. 6 one can see that, in contrast with the noninteracting problem, the flow lines on the (x,v) projection can now cross each other. Therefore, the focal fixed point of Eq. (7) is transformed now to the so-called ''focal-saddle'' singular point (recall that the phase space of the many-body system is $2N$ dimensional). Such a singular point is a typical configuration which produces dynamic chaos in systems with more than two degrees of freedom. The chaotic nature of the attractor of Fig. 6 was checked numerically by calculating the largest Lyapunov exponent which has been found to be positive. Additionally, in Fig. 7 we plot the discrete mapping of velocities for the attractor of Fig. 6 $v_i[k]\to v_i[k+1]$ with

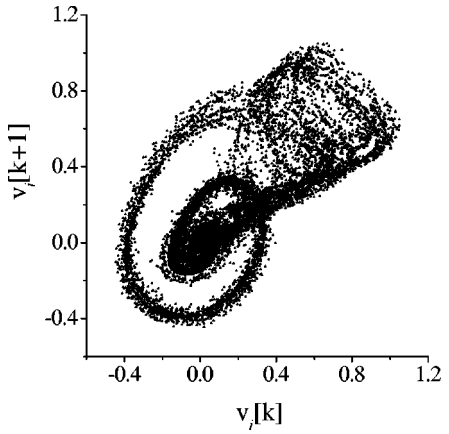

FIG. 7. Stroboscopic map of velocities $v_i[k]\to v_i[k+1]$ for the attractor of Fig. 6.

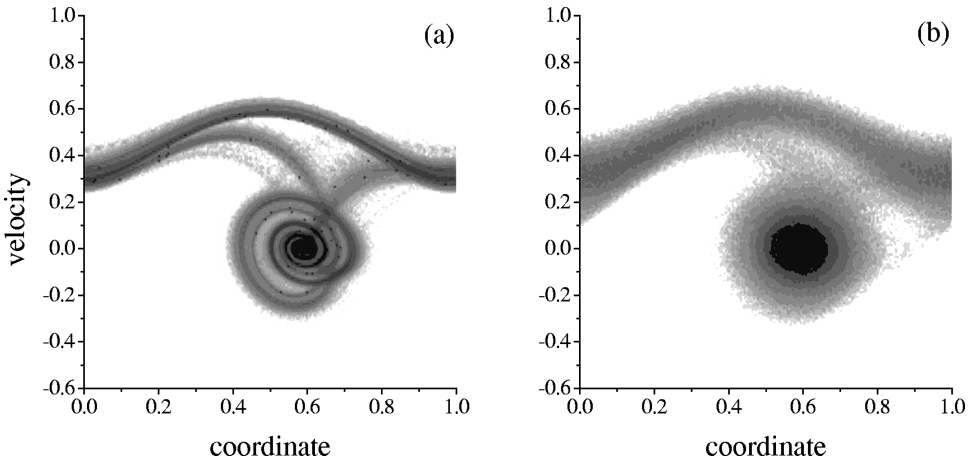

FIG. 8. Gray-scale map for continuous many-body density $W(x_i,\dot{x}_i;t\to\infty)$ calculated for (a) $T=0$ and (b) $T=0.1$. Other parameters are the same as in Fig. 6.

the discrete time step $t_{k+1}=t_k+\tau_0$ ($\tau_0=2\pi$ is the period of oscillations at the minimum of the substrate potential at $F=0$). Figure 7 clearly demonstrates a chaotic nature of the attractor. Recalling now that the system under consideration is dissipative and, therefore, a phase volume Ω of the system must decrease with time, $d\Omega\{x_i,\dot{x}_i\}/dt\propto-\eta\Sigma_i|\dot{x}_i|$, we come to the conclusion that *the $T=0$ state with traffic jams corresponds to the strange attractor* of the system. (Notice that every strange attractor contains a countable set of regular trajectories, so one can always find an initial configuration leading to the regular behavior. However, the set of initial configurations leading to the stochastic behavior is uncountable.)

To study the stability of this strange attractor with respect to temperature fluctuations, let us rewrite Eq. (1) as a set of two stochastic equations

$$\dot{x}_i=v_i, \tag{8}$$

$$\dot{v}_i=-\eta v_i-\sin x_i+F-\frac{\partial}{\partial x_i}[V(x_{i+1}-x_i)+V(x_i-x_{i-1})]+\delta F_i(t) \tag{9}$$

or, in a compact form for the variables ξ_j, $j=1,\ldots,2N$, where $\xi_{2i-1}\equiv x_i$ and $\xi_{2i}\equiv v_i$, as

$$\dot{\xi}_i=-h_i(\{\xi_i\})+\sum_j g_{ij}\delta F_j(t). \tag{10}$$

The system (10) can alternatively be rewritten in terms of the Fokker-Planck equation (FPE) for continual (macroscopic) variables y_i

$$\frac{\partial W}{\partial t}=\left[-\sum_{i=1}^{2N}\frac{\partial}{\partial y_i}D_i^{(1)}(\{y\})+\sum_{i,j=1}^{2N}\frac{\partial^2}{\partial y_i\partial y_j}D_{ij}^{(2)}(\{y\})\right]W, \tag{11}$$

where $W(\{y\};t)$ is the distribution function. The drift vector $D_i^{(1)}$ and the diffusion tensor $D_{ij}^{(2)}$ in Eq. (11) are coupled with the coefficients of Eq. (10) by the following relationships [8,9]:

$$D_i^{(1)}(\{y\})=h_i(\{y\}),\quad D_{ij}^{(2)}(\{y\})=\sum_{k=1}^{2N}g_{ik}g_{kj}. \tag{12}$$

The only method for a numerical solution of a many-body FPE is to employ the Monte Carlo technique. For Eq. (11), this technique reduces to the solution of the set of Langevin equations (10). We used the following technique. Starting with an appropriate initial configuration, first we waited a transient time $t_{\rm tr}$ until the system reaches a steady state. Then, for discrete time moments $t_k=t_{\rm tr}+k\Delta t$ we calculated the numbers of atoms within different small phase volumes $\{\xi_i,\xi_i+\Delta\xi_i\}$ and accumulated the counts during an averaging time $t_{\rm av}$. The stationary distribution function $W(\{y\})$ is just proportional to these counts, so we are left to normalize it according to the equation $\int dy_i\cdots dy_N W(\{y\})=1$.

The parameters of the described procedure have to be chosen numerically in order to result in negligibly small further corrections to the density $W(\{y\})$. In the simulation we used the parameters $t_{\rm tr}=30\tau_0$, $t_{\rm av}=500\tau_0$, $\Delta t=0.02\tau_0$, and the phase space was discretized with $\Delta x=0.005$ and $\Delta v=0.01$. As the initial configuration we used a random distribution of atomic coordinates and velocities, although we checked that the final distribution does not depend on the initial one. To test this technique, first we calculated the distribution function for the system of noninteracting atoms and compared the result with the one obtained by a numerical solution of the one-particle Fokker-Planck equation on a 256×256 grid. The distribution functions calculated by both methods were found to coincide; the corresponding function is shown in Fig. 5(b).

The projection of the probability density $W(\{y\};t)$ onto the plane (x,v) for the chain of interacting atoms with the same model parameters as those of Fig. 6 is presented in Figs. 8(a) and 8(b) for $T=0$ and $T\neq0$, correspondingly. One can see that, first, the many-body attractor exhibits a chaotic behavior at $T=0$ already, and second, both the channels connecting the running and locked states persist under applying a thermal noise. Thus, we conclude that *the traffic-jam state remains stable at nonzero temperatures*, at least for small enough T (this statement is also confirmed by the simulation presented in the next section).

III. PHASE DIAGRAM

As was mentioned in the Introduction, for a slow changing of the external force the transition to the state with jams is not observed for the standard FK model, but does exist for the exponential interatomic interaction. Thus, the second im-

portant question emerges: for what system parameters might one expect the transition from the homogeneous state to the inhomogeneous traffic-jam regime? To find an answer, we made a series of simulations for different model parameters.

First, the existence of jams could be expected only for an underdamped system, because the system must have two different states for atoms, the running state and the locked state, and this is possible only when $\eta < \eta_c$. Thus, the external damping coefficient η is an important parameter of the model. Having this in mind, we modified the simulation algorithm used in the Introduction, in the following way: for given values of g, β, and T, first we prepared the initial configuration by relaxing the equidistant configuration at $F=0$ and $T=0$, then we applied the dc force F and the Gaussian random force corresponding to the temperature T, and allowed for the system to reach a steady state, waiting a time $t_{\mathrm{tr}}=100\tau_0$. At the beginning, the external damping was taken to be large, $\eta=1$ (recall that the characteristic frequency of atomic vibrations is $\omega_0=1$). Next, we decreased the damping coefficient η with small steps (each new value of η was obtained from the previous one by dividing over 1.0183, i.e., we made 128 steps for the variation of η from $\eta=1$ to $\eta=0.1$), and at each step we first waited the time $100\tau_0$ to allow the system to reach a new steady state, and then during the next time period of $t_{\mathrm{av}}=100\tau_0$ we measured system characteristics such as the average system velocity and the velocity correlation function. In the simulation we used the parameters $F=0.5$, $N=256$, $T=0.1$, and $g=0.1$. The dependence $B(\eta)$ is similar to that of $B(F)$ described above: when η decreases, the system passes from the low-mobility locked state (LS) to the high-mobility running state (RS). For the harmonic interaction, this transition occurs in one step, and the correlation functions exhibit a peak just at the transition point. For the exponential interaction, the transition proceeds, on the contrary, in two steps. First the system passes to an intermediate state characterized by a shell with $0<B<B_f$, and only then with a further decrease of η is the running state with $B\approx B_f$ finally reached. As we checked by analyzing the atomic trajectories, this intermediate state always corresponds to the steady state with jams. At the same time the correlation function $K_1(\eta)$ exhibits two peaks, one at the transition to the inhomogeneous traffic-jam state (JS), and the second at the transition to the running state. From the definition (5) one can see that the value of K_1 should be proportional to the number of jams in the system because the velocities of nearest-neighboring atoms may differ essentially only at the boundaries separating the running and jam domains. Therefore, we can use the fact that two peaks on the dependence $K_1(\eta)$ exist as an indication of the jam state, while the positions of these peaks show the parameter range for JS existence.

To study the role of the anharmonicity of the interaction, we made a series of runs for different values of the parameter β, keeping at the same time the value of the elastic constant g fixed, so that the limit $\beta\to 0$ corresponds to the harmonic interaction (the standard FK model), while the limit $\beta\to\infty$ describes a hard-core gas. The simulation results are shown in Fig. 9 for the $B(\eta)/B_f(\eta)$ dependences [recall $B_f(\eta)=\eta^{-1}$] and in Fig. 10 for $K_1(\eta)$. Notice that the primary dependences occur to be too noisy, so we had to smooth them by a standard technique before plotting them in the figures. Finally, in Fig. 11 we plot the phase diagram on the (η,β) plane by extracting the positions of maxima of $K_1(\eta)$ for every value of β.

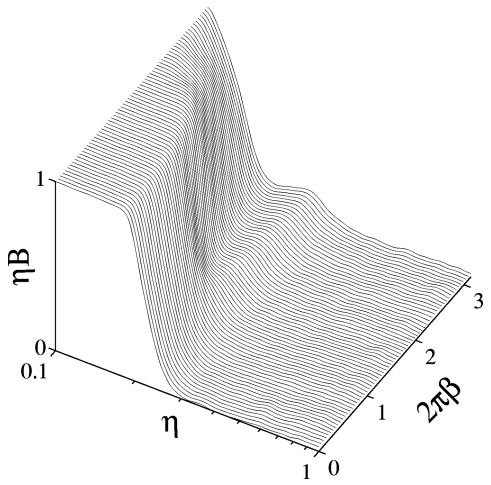

FIG. 9. The dimensionless mobility B/B_f as a function of η for different values of the exponent β at a fixed value of the elastic constant g. $N=256$, $g=0.1$, $F=0.5$, and $T=0.1$.

The simulation results provide the answer we were looking for: the transition to the steady state with jams emerges for the exponential interaction (2) for $\beta > a^{-1}$ only. Because $r=\beta^{-1}$ corresponds to an effective radius of the interatomic interaction, this result means that for a slow variation of the system parameters the jam states appear only if the atoms occupying the next-nearest-neighboring wells of the substrate potential are almost not interacting.

Thus, we come to the conclusion that the transition to the traffic-jam state emerges only for short-range interatomic interactions when the radius of the interaction is smaller than the period of the external periodic potential, and only for small damping coefficients in an interval just preceding the transition to the running state. Other parameters of the model such as the temperature or the elastic constant, are not essential for the problem under study. In particular, recall that in Sec. II we observed the traffic-jam state for even zero tem-

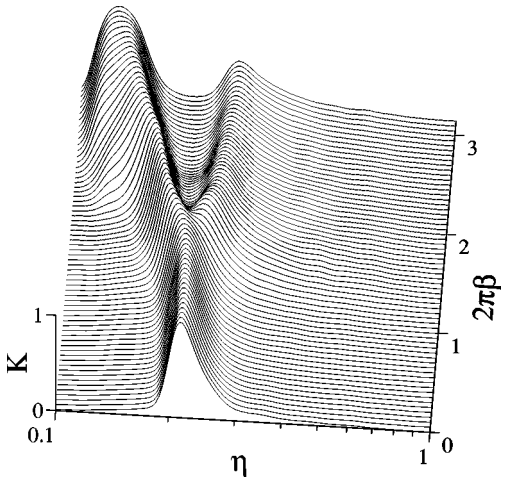

FIG. 10. The same as in Fig. 9 for the velocity correlation function K_1. For a better view, every dependence $K_1(\eta)$ is normalized on its own maximum.

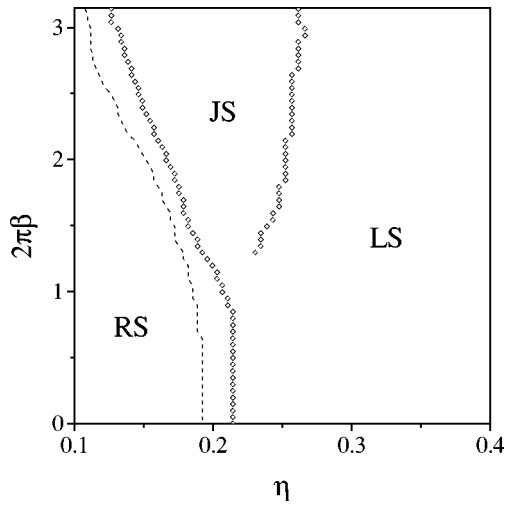

FIG. 11. Phase diagram on the (η,β) plane. LS is the locked state, JS is the steady state with jams, and RS is the running state. Diamonds correspond to maxima of $K_1(\eta)$ and the dashed curve corresponds to the $B(\eta)=0.9B_f$ threshold. The parameters are the same as in Fig. 9.

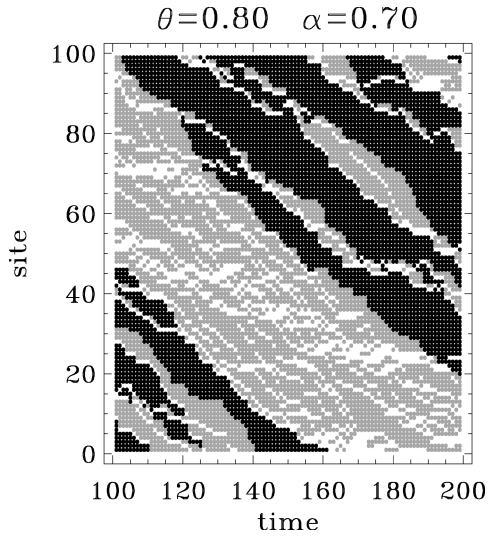

FIG. 12. Evolution of the lattice-gas model. Immobile atoms are shown as black circles and running atoms as gray circles. Time is measured in Monte Carlo attempts per site. The system size is $M=10^3$, $\theta=0.8$, and $\alpha=0.7$.

perature, although in this case we had to start with a random distribution of atoms as the initial configuration.

IV. GENERALIZED LATTICE-GAS MODEL

As was shown in Sec. III, the transition to the traffic-jam regime emerges only in the case of short-range interatomic interactions. Therefore, let us try to model the traffic-jam behavior with the help of a lattice gas (LG), where atoms occupy the sites with at most one atom per site and jump stochastically to vacant nearest-neighboring sites. Let us assume that an atom may jump to the right with the probability α and to the left with the probability $1-\alpha$, where $\frac{1}{2}<\alpha\leqslant 1$. Recalling the FK model, the probability of a jump to the right at small external forces is $\alpha\approx(1+e^{-aF/T})^{-1}$, so the parameter α in the lattice-gas model plays the role of the driving force in the FK model. Such a variant of the LG model is known as the partially asymmetric exclusion model [10,11]. The $\alpha=1$ variant of this model, called the totally asymmetric exclusion model, has recently been solved exactly [12].

The underdamped FK model has, however, one more important aspect: an atom after the jump does not stop in the next potential well but continues to move until it meets a stopper, e.g., an immobile atom in front of itself. To incorporate this feature into the lattice gas model, we assume that an atom may be in two different states: the ''immobile'' state, in which it jumps as usual in the LG model, and the ''running'' state, in which the atom always jumps to the right provided the right-hand site is empty. The important aspect of the model is that an atom can change its state from the immobile state to the running state and vice versa: the immobile atom is in the running state after a jump to the right, and the running atom becomes immobile after a collision with an immobile atom. Such a model may be called the traffic-jam LG model, because the atoms behave similar to cars in a one-lane road.

Thus, the simplest model may be introduced as follows. Consider a one-dimensional lattice of length M with periodic boundary conditions. Each site is either occupied by one atom or is empty. Let N be the total number of atoms and let the dimensionless concentration be defined as $\theta=N/M$. Each atom may be in one of two states, the immobile state or the running state. The system evolves in time according to the sequential dynamics, i.e., atoms jump independently and randomly according to the following rules.

(1) At each time step $t\rightarrow t+1$, one chooses a site i at random.

(2) If this site is occupied by an immobile atom, it jumps to the site $i+1$ (if this site is empty) with probability α or it jumps to the site $i-1$ (if the left-hand site is empty) with probability $1-\alpha$ as in the partially asymmetric exclusion model. After a jump to the left the atom remains in the immobile state, while *after a jump to the right the atom is in the running state.*

(3) If the atom in the chosen site i is in the running state, it jumps to the right provided the right-hand site is empty, and remains in the running state. Otherwise, if the site $i+1$ is not empty, the atom in the site i remains in the running state if the right-hand site is occupied by the running atom or *becomes immobile if the site $i+1$ is occupied by the immobile atom.*

A typical picture of system evolution started from a random distribution of immobile atoms is shown in Fig. 12. As seen, from the very beginning the system splits into compact domains of immobile and running atoms. The immobile domains (jams) are characterized by the local atomic concentration $\theta_s=1$. The jams are separated by running domains characterized by a local concentration $\theta_r<\theta$. One can see that Fig. 12 looks similar to the trajectories in Fig. 3 of the FK model.

To characterize the system state, let us introduce the dimensionless ''mobility'' B as the ratio of the number of running atoms N_r to the total number of atoms N,$B=N_r/N$. The dependences of B on α for different values of θ are shown in Fig. 13. To calculate B analytically, let us suppose

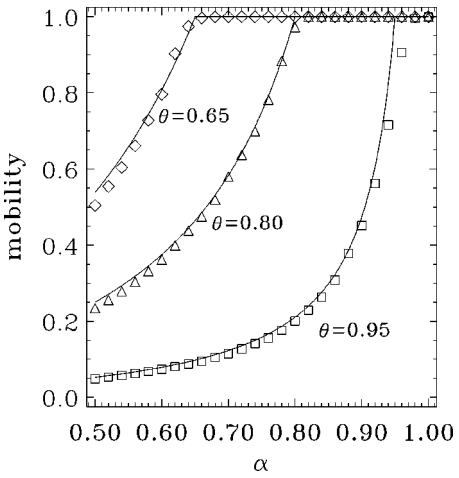

FIG. 13. Mobility B as function of the jump probability α for different values of θ: $\theta=0.65$ (diamonds), $\theta=0.80$ (triangles), and $\theta=0.95$ (squares). Each data point is an average over 5×10^3 attempted jumps per site. The averaging was started after 5×10^3 MC steps. The data were averaged additionally over 28 independent runs. The system size is $M=10^3$. Solid curves are the predictions of Eq. (16).

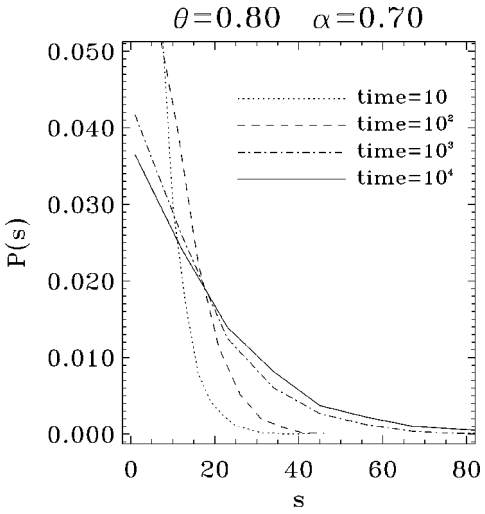

FIG. 14. Distribution of jam's sizes at different times: $t=10$ (dotted curve), $t=10^2$ (dashed curve), $t=10^3$ (dot-dashed curve), and $t=10^4$ (solid curve). The chain's length is $M=10^3$, $\theta=0.8$, and $\alpha=0.7$. The histograms were averaged over 100 independent runs.

that there is only one jam in the chain. Let this jam have length s. Because the local concentration in the jam is $\theta_s=1$, we can apply the following simple arithmetic [4]:

$$s+N_r=N, \quad s+M_r=M, \tag{13}$$

where M_r is the length of the running domain (RD). Taking into account that $N_r=M_r\theta_r$ and $N=M\theta$, we obtain $s=M(\theta-\theta_r)/(1-\theta_r)$, so that the mobility is equal to

$$B=\frac{\theta_r(1-\theta)}{(1-\theta_r)\theta}. \tag{14}$$

Evidently, Eq. (14) should be valid as well for the steady state with any number of jams provided θ_r corresponds to the mean atomic concentration in the RD's.

According to the rules accepted above for the LG model, the most left site of any RD is always empty (this is clearly seen in Fig. 12). Therefore, the running domain grows from its left-hand side at the rate α due to the injection of new atoms from the left-hand-side neighboring jam. At the right-hand side of the RD, the atom which occupies the most right site of the RD leaves the RD and joins itself to the neighboring right-hand-side jam. Thus, the RD shortens from the right-hand side at the rate p_r, where p_r is the probability that the farthest right site of the RD is occupied. Clearly, in the steady state $p_r=\alpha$. Neglecting by a possible deviation of the RD concentration at its right-hand side from the mean value θ_r, we may take approximately

$$p_r\approx\theta_r, \tag{15}$$

and finally we come to the expression

$$B\approx\frac{\alpha(1-\theta)}{(1-\alpha)\theta}, \quad \alpha<\theta. \tag{16}$$

For $\alpha>\theta$ the jams all disappear, and $B=1$ in the steady state. The dependences (16) shown by solid curves in Fig. 13, describe the simulation results with good accuracy.

Now let us dwell on the steady state in more detail. A jam of length s loses atoms from its right-hand side at the rate α, and it receives new atoms to the left-hand side at the rate p_r. These two rates are equal to one another in the steady state, so in average $\langle\dot{s}(t)\rangle=0$. However, because of the randomness of joining and losing events, the value $s(t)$ will exhibit random walks, i.e., at long times, $t\gg1$, $t'\gg1$, and $|t-t'|\gg1$, $s(t)$ should behave according to the equation

$$\langle[s(t)-s(t')]^2\rangle\approx2\alpha|t-t'|. \tag{17}$$

Thus, at $\alpha<\theta$ *the infinite system has no steady state at all*. Indeed, when a jam reaches the size $s=0$, it disappears forever, while the motion of $s(t)$ to higher values is not restricted in the infinite system. The distribution of jam sizes $P(s)$ continuously changes with time shifting to larger and larger values as shown in Fig. 14, so that instead of the name ''steady state'' it is more reasonable to use the name ''quasisteady state'' or ''coarsening state.'' However, the mobility of the coarsening state does not change with time [13]. According to Eq. (16), B is determined by the system parameters only and does not depend on the distribution $P(s)$.

The transition to the running state in this simple LG model is of second order in the sense that the current changes continuously at the point $\alpha=\theta$. However, the simplest model exhibits a trivial hysteresis: when *all* atoms come into the running state, this state then remains unchanged forever, even if α is changed back to lower values. In this sense the transition may be considered as first order.

Keeping in mind that we want to describe qualitatively the behavior of the FK model, let us now improve the LG model to make it more realistic, allowing the running atoms to spontaneously change their state back to the immobile state with some probability $\gamma<1$. Namely, let us slightly modify the third rule of the system evolution in the following way: (3′) If the atom in the chosen site i is in the running

state, it comes to the immobile state with the probability γ, or evolves according to the rule (3) with the probability $1-\gamma$.

To describe this variant of the LG model analytically, we will use the mean-field (MF) approach and suppose that all running domains are characterized by the same concentration θ_r. In addition, we also assume that the probability of occupation of the most right site of the running domain is equal to θ_r as above in Eq. (15). With these assumptions, a jam of length s increases ($s \to s+1$) with the rate θ_r, and decreases ($s \to s-1$) with the rate α. Denoting by $n_s(t)$ the number of jams of length s at time t, we can write the following kinetic equation for $n_s(t)$:

$$\dot{n}_s = -\alpha n_s - \theta_r n_s + \theta_r n_{s-1} + \alpha n_{s+1}, \quad s \geqslant 2. \tag{18}$$

Equation (18) has a simple steady-state solution $n_s = n_1(\theta_r/\alpha)^{s-1}$. The distribution of jam sizes is described by the expression

$$P(s) \equiv \frac{n_s}{J} = \frac{\alpha - \theta_r}{\alpha}\left(\frac{\theta_r}{\alpha}\right)^{s-1}, \tag{19}$$

where $J = \Sigma n_s = n_1\alpha/(\alpha-\theta_r)$ is the total number of jams. The total number of immobile atoms is equal to $N_s = \Sigma s P(s) = n_1\alpha^2/(\alpha-\theta_r)^2$. Applying now the same arithmetic as above in Eq. (13), we can find the mobility

$$B = (1+p)^{-1} \tag{20}$$

and the average concentration in the running domains

$$\theta_r \equiv \frac{N_r}{M_r} = \frac{\theta}{1+p-p\theta}, \tag{21}$$

which depend on the parameter p defined as

$$p = \left(\frac{n_1}{N_r}\right)\left(\frac{\alpha}{\alpha-\theta_r}\right)^2. \tag{22}$$

To complete the set of equations, we must have a kinetic equation for $n_1(t)$ which plays the role of boundary condition for Eqs. (18). It may be written as

$$\dot{n}_1 = \gamma N_r + \alpha n_2 - \alpha(1-\theta_r)n_1 - \theta_r n_1. \tag{23}$$

The first term on the right-hand side of Eq. (23) describes the creation of immobile atoms from the running atoms, and the other terms have the same meaning as in Eq. (18) except that now $n_0 = 0$ and the rate of the disappearance of one-atomic jams is not α but $\alpha(1-\theta_r)$, because these jams are emerging mostly inside the running domains and the condition that the next-neighboring site to the right of the one-atomic jam is empty is not valid anymore. The steady-state solution of Eq. (23) is

$$n_1 = \gamma N_r/\alpha(1-\theta_r). \tag{24}$$

Substituting Eq. (24) into Eqs. (21),(22), we obtain an equation on θ_r

$$(\theta-\theta_r)(\alpha-\theta_r)^2(1-\theta_r) - \gamma\alpha\theta_r(1-\theta) = 0, \tag{25}$$

which may be easily solved numerically. As we checked, the MF dependences $B(\alpha)$ describe simulation results with high accuracy.

In the FK model, the rate of spontaneous transition to the immobile state depends on the external force F, i.e., on the inclination of the periodic substrate potential: it is zero for $F > F_f$ and increases with F decreasing in the region $F < F_f$. In the lattice-gas model this means that γ must be zero at $\alpha = 1$ but it has to increase when α decreases. For concreteness, one may take the simple expression $\gamma = \gamma_0(1-\alpha)^2$, where γ_0 is a model parameter and the square dependence is chosen in order to avoid an unphysical peculiarity in the $\alpha \to 1$ limit.

The model (3′) has a true steady state and does not exhibit irreversibility anymore; the $\gamma \neq 0$ condition totally kills the hysteresis. This is because in the LG model the probability of the spontaneous transition of an atom from the running state to the immobile state does not depend on the state of the surrounding atoms. This is true for the transition of an isolated atom, but is too crude an approximation for the FK system which we are trying to model. Indeed, when an atom inside a RD becomes immobile, it will be immediately pulled back to the running state by the running atoms behind it. This ''inertia'' effect cannot be described rigorously in the framework of a lattice-gas model. But let us try to simulate this effect qualitatively, modifying the third evolution rule in the following way.

(3″) In the case where a randomly chosen site i is occupied by a running atom and the site $i+1$ is occupied by an immobile atom, we will count the total number s of immobile atoms in the compact jam to the right of the bond $i--(i+1)$, and the number r of running atoms behind this bond in the compact running block, i.e., s is the distance from the bond $i-(i+1)$ to the first empty site in the positive x direction and r is the same distance in the negative x direction. Then the system is updated according to the following rule: if $r < s$, all $r+s$ atoms become immobile, otherwise (if $r \geqslant s$) all $r+s$ atoms ''belonging'' to the $i-(i+1)$ bond become running. In all other cases the system evolves similarly to the model (3′), i.e., if the site $i-1$ is empty, the atom either comes to the immobile state with the probability γ, or remains in the running state with the probability $1-\gamma$, jumping to the right provided the site $i+1$ is not occupied.

The simulation results for this generalized LG model are presented in Fig. 15. The main new feature of the model is that now we have a nontrivial hysteresis similar to that of the FK model. When α decreases starting from the $\alpha = 1$ value, the state without jams survives at values of α lower than θ before the RS jumps back to the state with jams. As seen from Fig. 15, the width of the hysteretic loop depends on the concentration θ, for higher values of θ the loop is wider. In addition, the width of hysteresis depends on the rate of α variation as seen in Fig. 16. The slower α is changed, the more narrow the hysteretic loop, so that for the adiabatically slow variation of α the hysteresis should disappear altogether. This means that the running state of the system at $\alpha < \theta$ is a metastable state characterized by a finite lifetime τ_r.

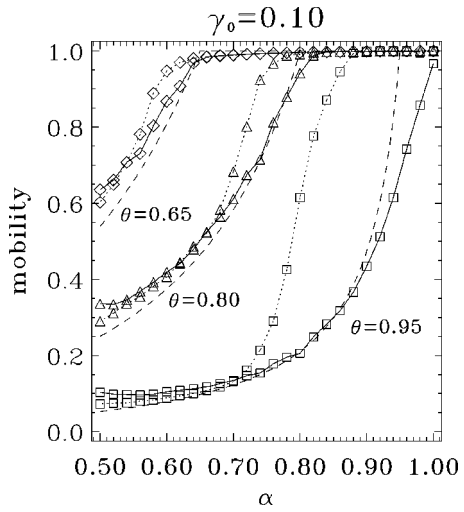

FIG. 15. Mobility $B(\alpha)$ for the generalized LG model for different values of θ: $\theta=0.65$ (diamonds), $\theta=0.80$ (triangles), and $\theta=0.95$ (squares). For each θ the simulation was started from the random configuration of immobile atoms at $\alpha=0.5$, then the final configuration of the previous step was used as the initial configuration for the next value of α. Solid curves correspond to the increasing of α, and the dotted curves, to its decreasing. Each data point is an average over 1.5×10^3 attempted jumps per site. The averaging was started after 1.5×10^3 MC steps. The data were averaged additionally over 30 independent runs. The system size is $M=10^3$ and $\gamma_0=0.1$. The dashed curves correspond to Eq. (16) of the simple LG model.

The distribution of lifetimes τ_r of the running state is shown in Fig. 17. To estimate the mean value of τ_r analytically, let us consider a state with a single jam of size s at time t. This jam will be killed in the next Monte Carlo (MC) step $t+1$, if just behind it there is a compact block of running atoms of a size $r\geqslant s$. In the RS the probability to have such a block of running atoms is θ^s. Thus, at the time $t+1$ the s-atomic jam will disappear with the probability θ^s, and it will survive till the next time step with the probability $1-\theta^s$. Therefore, in average the s-atomic jam will survive if $1-\theta^s\geqslant\theta^s$, or $s\geqslant s_0$, where the critical size s_0 is equal to $s_0=-\ln 2/\ln\theta$.

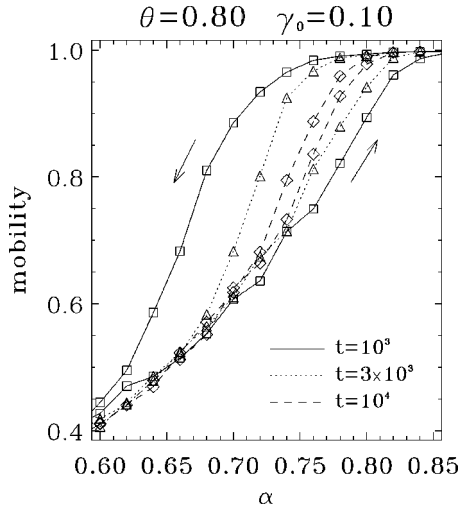

FIG. 16. Hysteresis in the generalized LG model for different simulation times. Squares and solid curve for an averaging over 0.5×10^3 MC steps per site; the averaging started after 0.5×10^3 steps. Triangles and dotted curve for an averaging over 1.5×10^3 steps; the averaging started after 1.5×10^3 steps. Diamonds and dashed curve for an averaging over 5×10^3 MC steps; the averaging started after 5×10^3 steps. The chain's length is $M=10^3$, $\theta=0.8$, $\gamma_0=0.1$, the data were averaged additionally over 30 independent runs.

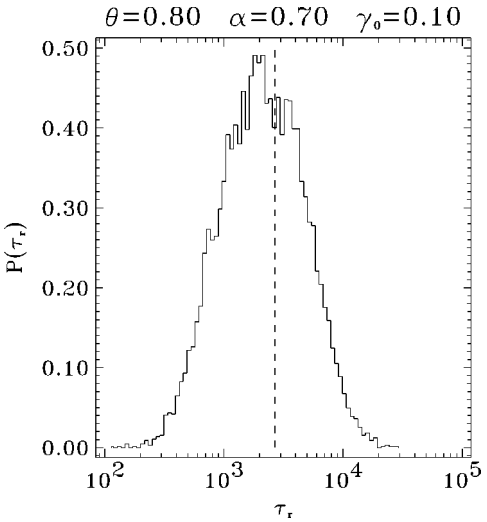

FIG. 17. Distribution of times τ_r of transition from the running state to the state with jams. The system size is $M=10^3$, $\theta=0.8$, $\alpha=0.7$, and $\gamma_0=0.1$. The hystogram was calculated with 8×10^3 points. Each simulation was started from the initial configuration of running atoms, then it was ''equilibrated'' at $\alpha=1$ during the time 10^3 MC steps, after that α was abruptly decreased to the value $\alpha=0.7$, and the simulation was stopped when B reached the value $B=0.9$ for the first time. The broken line shows the prediction of Eq. (26).

Now let us suppose that at the time $t-1$ the chain was in the running state, and calculate the probability that at the time t the chain has a jam of the size s_0. For one MC step, the number of newly created immobile atoms is γN (recall $N_r=N$ in the RS), so that the probability for a given site to be occupied by one immobile atom is $\gamma N/M=\gamma\theta$. Therefore, the probability that at a given place the s_0-atomic jam will appear is $(\gamma\theta)^{s_0}$. Taking into account now that for the transition to the JS the chain may have only one jam, we obtain that in a chain of length M the probability of the RS $\rightarrow$JS transition per one MC step is $M(\gamma\theta)^{s_0}$. Therefore, we come to the expression

$$\langle\tau_r\rangle=1/M(\gamma\theta)^{s_0}. \tag{26}$$

Although the estimation (26) is crude, it predicts the correct value of $\langle\tau_r\rangle$ for the model parameters used in Fig. 17 and demonstrates the right tendency for variation of the hysteretic loop with θ.

Equation (26) shows that the infinite system should have no hysteresis at all. This is simply the result of the one-dimensionality of the model. Indeed, at $\alpha<\theta$ for any small but finite probability of creation of the s_0-atomic jam, at least one jam will certainly be created per each time step, and this jam will cause the RS$\rightarrow$JS transition.

V. FOKKER-PLANCK APPROACH AND MEAN-FIELD THEORY

The numerical simulations of Sec. II have shown that the transitions between different steady states (the locked and running ones) take place at some critical value of the parameters of the system. From a qualitative point of view these transitions can be treated as some kind of specific phase transition between different dynamic states. Sharp transitions are found to survive at nonzero temperatures, at least within the accuracy of the numerical simulation. This essential feature of the system contrasts with the disappearance of bistability in the system of noninteracting particles at any $T>0$. To study this problem, it could be useful to find a continuous field description based on an effective energy functional in order to then use a standard approach of the theory of phase transitions (e.g., see Ref. [14]). The continuous many-body probability distribution W calculated above in Sec. II already provided us with a feeling of how to construct a reduced mean-field model. Namely, the idea is to find an effective Fokker-Planck or Langevin equation for some one- or two-particle function W, which will reproduce, at least qualitatively, the same behavior as the exact many-body model.

Keeping this in mind, let us complete the one-particle Langevin equation (6) by an ''integral'' (collective) interaction with all other particles, adding a new stochastic equation in the following way:

$$\dot{x}=v, \quad \dot{v}=-\eta v-\sin x+F+\zeta+\delta F(t), \tag{27}$$

$$\dot{\zeta}=\mu, \quad \dot{\mu}=-\eta\mu+(\langle v\rangle-v). \tag{28}$$

With the help of Eq. (28) we introduce an additional degree of freedom (an ''artificial atom'' with the same mass and damping constant as the real atoms of the FK chain) which has to describe qualitatively the motion of the center of mass of the system. In Eq. (27) we suppose that the motion of a given *reference* atom is perturbed by a force ζ due to some averaged interaction with this ''artificial atom,'' i.e., with all other atoms of the chain. In turn, the value of ζ is assumed to be proportional to the deviation of velocity of the reference atom from the mean chain's velocity $\langle v\rangle$. Indeed, in a uniform state, when all atoms move with the same velocity and the atoms are arranged equidistantly, the interactions of the given atom with its neighbors, $-\partial/\partial x_i[V(x_{i+1}-x_i)+V(x_i-x_{i-1})]$, cancel each other. Therefore, the interparticle interaction will perturb the motion of the reference atom only when its velocity v deviates from the mean value $\langle v\rangle$ and thus destroys the system uniformity. In a rigorous approach, the averaging here should be performed over neighboring particles inside a correlation distance $r\sim\beta^{-1}$. In a mean-field approximation, however, the value of $\langle v\rangle$ is calculated over the whole phase volume Ω,

$$\langle v\rangle=\frac{\int_\Omega dx\ dv\ d\zeta\ d\mu[v W(x,v,\zeta,\mu;t)]}{\int_\Omega dx\ dv\ d\zeta\ d\mu\, W(x,v,\zeta,\mu;t)}, \tag{29}$$

so it depends on time t only. Numerical solution of Eqs. (27)–(29) shows that such a simple interaction $(\langle v\rangle-v)$ is already sufficient to restore the channels connecting the running and locked states in the system. Indeed, the projection of density W onto the subspace (x,v), calculated for the system (27)–(29) at $T=0$ and shown in Fig. 18, looks similar to the distribution of Fig. 8(a) obtained within the exact approach. Note, however, that the system (27)–(29) was not deduced from the complete set of Langevin equations (1) but rather was guessed, and the only justification of its introduction is the similarity of Figs. 8(a) and 18.

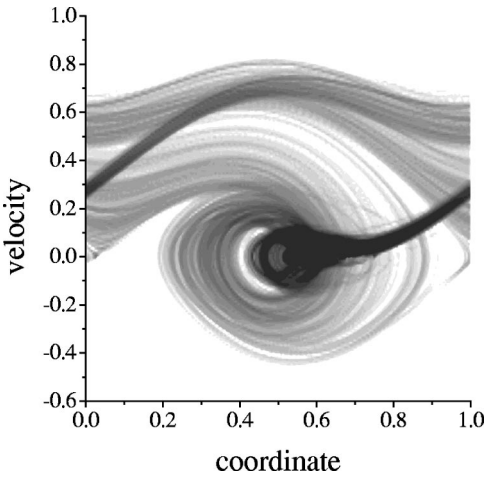

FIG. 18. The result of numerical solution of two coupled equations (27) and (28) at $T=0$ for the same model parameters as in Fig. 6. The projection of density $W(x,v;t)$ onto subspace (x,v) is shown by a gray-scale map.

However, even the system of two coupled Langevin equations (27), (28) is too complicated for an analytical description. To reduce the number of equations, recall that in the mean-field approach we can usually only restrict ourselves to a vicinity of steady states. As we tested numerically, small perturbations of the velocity v of the running or locked states result in a linear variation of the value ζ,

$$\zeta\simeq\alpha_{r,l}(\langle v\rangle-v), \tag{30}$$

where the coefficients $\alpha_{r,l}$ were found to be $\alpha_r\approx 3.3$ and $\alpha_l\approx 0.7$ for the running and locked states, respectively. Thus, we may omit Eq. (28) and substitute Eq. (30) into Eq. (27). In the result we obtain the equations

$$\dot{x}=v, \quad \dot{v}=-\eta_{\rm eff}v-\sin x+F_{\rm eff}(\langle v\rangle)+\delta F(t), \tag{31}$$

where in the vicinity of the locked state we have to take $F_{\rm eff}(\langle v\rangle)=F+\alpha_l\langle v\rangle$ and $\eta_{\rm eff}=\eta+\alpha_l$, while in the vicinity of the running state we should put $F_{\rm eff}(\langle v\rangle)=F+\alpha_r\langle v\rangle$ and $\eta_{\rm eff}=\eta+\alpha_r$. Note that the linearized Eq. (31) is valid only in the vicinity of steady states and was derived for the investigation of stability of these states. Equation (31) corresponds to the following Fokker-Planck equation:

$$\frac{\partial W(x,v;t)}{\partial t}=\left[-\frac{\partial}{\partial x}v+\frac{\partial}{\partial v}\left(\eta_{\rm eff}v+\sin x-F_{\rm eff}(\langle v\rangle)+\eta_{\rm eff}T_{\rm eff}\frac{\partial}{\partial v}\right)\right]W(x,v;t), \tag{32}$$

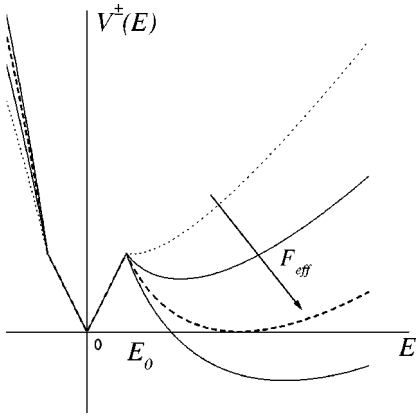

FIG. 19. The family of effective potentials $V^{\pm}(E)$ for different values of the effective force $F_{\rm eff}$. The dotted curve is for small force $F_{\rm eff}$ corresponded to the spinodal, when nontrivial minimum of the potential $V^{+}(E)$ disappears. The dashed curve corresponds to the binodal, when energies of locked and running states are equal one another ($F_{\rm eff}=F_{\rm crit}$).

where $T_{\rm eff}=T\eta/\eta_{\rm eff}$. The mean-field equation (32) takes into account the interaction between particles in a self-consistent way via the nonlinear term $-\partial F_{\rm eff}(\langle v\rangle)/\partial v$.

Recall that in this section we are looking for an approximate description of stationary states and transitions between them. For this purpose we have to find some effective energy functional. However, as is known from the general theory of FPE [8], such an effective potential can be defined at least in the low-friction limit, i.e., for the most interesting case of the problem under investigation. This limit corresponds to the case when both η and F are going to zero while their ratio $\tilde{F}_{\rm eff}(\langle v\rangle)=F_{\rm eff}(\langle v\rangle)/\eta_{\rm eff}$ remains finite. In the $\eta\to 0$ limit the atomic trajectories are close to those of constant energy $\epsilon=\frac{1}{2}v^2+1-\cos x-xF_{\rm eff}$ and the energy becomes the only relevant variable of the problem. A steady-state solution of Eq. (32) can now be written as an effective Boltzmann distribution

$$W(x,v;t)\propto\exp[-V^{\pm}(E)/T_{\rm eff}], \tag{33}$$

where $E=\epsilon\ \mathrm{sgn}(v)$, and the effective potential $V^{\pm}(E)$ is

$$V^{\pm}(E)=|E| \tag{34}$$

for $|E|\leqslant E_0$, while for $|E|>E_0$ it has different definitions for positive and negative velocities:

$$V^{\pm}(E)=|E|-\mathrm{sgn}(v)\tilde{F}_{\rm eff}(\langle v\rangle) \times\int_{E_0}^{|E|}\frac{dE'}{\int_0^{2\pi}dx\sqrt{2[E'-(1-\cos x)]}}. \tag{35}$$

The family of effective potentials $V^{\pm}(E)$ for different values of the effective external force $F_{\rm eff}$ is shown in Fig. 19.

In the approximate approach of Eqs. (32)–(35) the dependence of the effective force $F_{\rm eff}$ on the averaged velocity $\langle v\rangle$ is the only ''memory'' about interparticle interaction of the primary system. The value of $\langle v\rangle$ is in turn determined by the total momentum of the system and depends self-consistently on its initial state. This allows us to give a qualitative explanation of why the bistability of running and locked states is much more strong for the system of interacting particles compared to the noninteracting ones.

As seen from Fig. 19, there is some critical force $F=F_{\rm crit}$ at which the two minima of the potential $V^{\pm}(E)$, one at $E=0$ and the other at $E\neq 0$, are equal to one another (in Fig. 19 this binodal state is shown by a dashed curve). If we start from the locked state $\langle v\rangle|_{t=0}=0$ and apply a force F lower than the critical one $F<F_{\rm crit}$ (in the locked state $F_{\rm eff}=F$), so that the two minima coexist, but the trivial minimum is lower than the nontrivial one, the locked state should be more stable under temperature fluctuations (compared to the noninteracting system) due to the inequality $T_{\rm eff}\equiv T\eta/(\eta+\alpha_1)<T$. On the other hand, if the system is already in the running state, then $F_{\rm eff}=F+\alpha_r\langle v\rangle>F$, and one may have $F_{\rm eff}>F_{\rm crit}$ even for $F<F_{\rm crit}$. Moreover, if $\langle v\rangle|_{t=0}$ is large, the nontrivial minimum of the potential $V^{\pm}(E)$ may be deep enough to prevent any thermally activated escape of atoms from the running state during exponentially long times, and for any small (but finite) rate of variation of the dc force F the system should exhibit hysteresis.

Finally, let us discuss a close analogy of the self-stabilization of running and locked states which was observed in simulation and described above in the mean-field model with the stabilization of ordered states in thermodynamics. When a system is in the thermodynamic equilibrium state and the size of the system tends to infinity (and also if the interaction is long ranged enough), a phase transition between different ordered states is only possible due to the nucleation process [14]. Mesoscopic fluctuations (domains of a new state emerging near the transition point) collapse before they overcome some critical size, and only when one of the system parameters (e.g., temperature, magnitude, or correlation length of the interaction) reaches its critical value does the critical nucleus of the new phase start to appear. Then, the overcritical nucleus expands and initiates the transition of the whole system to the new state. A very similar nucleationlike scenario is observed in the *nonequilibrium* system studied in the present work. For example, in Fig. 20 we plot the phase pattern for the state close to the transition to the jam state ($g\to g_c$, $g<g_c$). Figure 20 was calculated for a slightly modified model: instead of Eq. (2), we used the interaction potential $V(x)=V_0e^{-\beta|x|}$, thus allowing the running atoms to pass over the locked ones. In this case one can have both running and locked states simultaneously. Below the transition point these states are separated from one another, but there are mesoscopic undercritical fluctuations which play the role of ''precursors'' for generation of ''traffic jams'' when the parameters of the interaction go to the critical values.

VI. CONCLUSION

We have shown with the help of a numerical simulation that the driven one-dimensional FK model exhibits hysteresis and the existence of traffic-jam states. Basing on the simulation we proposed two simple models which allow us to describe both these phenomena analytically. The first model is a generalization of the lattice-gas model with two states of atoms. This traffic-jam LG model is characterized by a non-

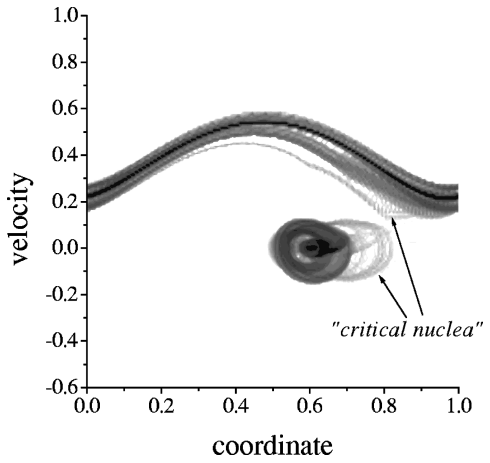

FIG. 20. Phase pattern for the state close to the transition ($g \simeq g_c$, $g<g_c$) for the following system parameters: $T=0$, $\eta=0.5$, $\beta=1/\pi$, $F=0.3$, $g=0.066$, and $\theta=2/3$. Both running and locked states are splitt and contain mesoscopic fluctuations (''critical nuclea'') of the phase with traffic jams.

linear dependence of the mobility on the jump probability, exhibits hysteresis, and describes the organization of immobile atoms into compact domains (jams). At the same time, as it is much simpler that the FK model, the LG model allows us to simulate much larger systems on a much longer time scale. In addition, we developed the MF theory for this LG model, which describes the kinetics of traffic jams and explains the simulation results with reasonable accuracy. Moreover, the generalized version of this model even exhibits hysteresis and allows us to estimate the probability of the transition from the running state to the jam state. The second model is based on the Fokker-Planck approach to the FK model and also uses the MF approximation. With its help we explained the stability of the steady states of the FK model. Finally, we can formulate, at least qualitatively, the answers to the questions that were asked in the Introduction.

Hysteresis does exist in the *underdamped* one-dimensional FK for any *finite* rate of force changing (and, strictly speaking, for any large but *finite* system). This statement is quite trivial because the same is true for a single driven Brownian particle in the periodic potential. However, in the system of interacting atoms the hysteretic loop is much larger and should survive at much higher temperatures. Indeed, due to concerned motion of atoms in the FK model, a single atom cannot exhibit bistability; the system must be transformed from one steady state to another as a whole. When the chain is in the low-mobility state, this state is more stable (compared to the noninteracting system) because of the effective decrease of temperature $T_{\text{eff}}<T$; local fluctuations with high-velocity atoms are suppressed due to the interatomic interaction. The transition to the running state begins only when the force F reaches the critical threshold F_f and the motion of topological excitations (kinks) becomes unstable (see details in Ref. [6]). On the other hand, if the system is in the running state and the force is then decreased, the RS remains stable because local fluctuations with low-velocity atoms (jams) are suppressed again due to the interaction. The effective driving force F_{eff} in the RS is larger than F, and the transition to the LS may only begin when a jam of the critical size (which may be mesoscopically large for a strong interatomic interaction) appears for the first time.

Traffic jams do appear in the *underdamped* FK model with *anharmonic* interaction just before the transition to the running state. We can formulate the following conditions which have to result in the traffic-jam behavior in the driven one-dimensional system.

(i) It must be an external (substrate) potential. In the present work we studied the case of a periodic potential, but a random external potential should lead to the traffic-jam scenario as well.

(ii) The motion must be underdamped; the particles should have two different states, the locked state and the running state (for the FK model this corresponds to frictions $0\leqslant\eta<0.56$, in the case of $\eta=0$ the ''intrinsic'' friction plays the role of damping). In the FK model the bistability exists due to the inertia of atoms. In the FP approach the same is due to memory effects; in the LG-type model one has to introduce such a bistability artificially. In a general case, the mean free path of the particle after overcoming the barrier of the external potential, must be larger than the period of the substrate potential or the average interparticle distance, whichever is larger. Notice that at a given F, the total (external plus intrinsic) friction must be larger than some threshold value, because otherwise an avalanche leading to the transition to the RS begins before the jam state will emerge [5,6].

These two conditions are already sufficient for the existence of the traffic-jam state. Indeed, if one prepares by hand the initial configuration with a jam and then abruptly applies the driving force, this state may survive in the classical FK model even at nonzero temperatures. However, the simulation of the present work showed that the *transition* from the homogeneous state to the traffic-jam state at slow variation of model parameters takes place only if two more conditions are satisfied.

(i) It must be some randomness in the system. As we have shown, already the intrinsic chaos, which always exists due to the nonintegrability of the discrete FK model, is sufficient for the existence of the traffic-jam behavior (although in the $T=0$ case we had to start from a random initial configuration). The simplest way to introduce chaos into the system is to use Langevin motion equations with $T>0$; in this case the traffic-jam state emerges for any initial state. Of course, the temperature should not be too large. The thermal energy must be lower than the energy of interatomic interaction (otherwise the behavior will be the same as for the system of noninteracting atoms) and lower than E_0 (otherwise the behavior will be the same as for the system without external potential).

(ii) The interparticle interaction has to be anharmonic. As has been shown, already the hard-core potential, when the atoms do not interact at all except that they cannot occupy the same well of the substrate potential, is sufficient to produce the traffic-jam behavior. Thus, one might expect no transition to the traffic-jam state for the harmonic interatomic interaction. However, the situation is more subtle: there is no transition to the traffic-jam state for *atoms* in the standard FK model, but the *kinks* may still be organized in jams because for any short-ranged interatomic interaction the interaction between the kinks is always exponential.

Other parameters of the system are not crucial and would only change the parameter range of existence of the traffic-jam behavior. In the simulation we observed the traffic-jam states for different values of the elastic constant g as well as for different concentrations θ. Moreover, traffic jams exist even for the $\theta \sim 1$ case, although in this case not atoms but kinks are organized into jams.

Using the results of the present work, one can give a simple solution to how to avoid traffic jams: the particles (atoms in the FK model or cars in the one-lane road) should interact harmonically, i.e., they should try to keep an equidistant interval between themselves. Although this solution is quite trivial and has been well known empirically for a long time, the simple models considered in the present paper allow us to study this question *analytically* and *quantitatively*.

Finally, note that the model studied in the present work is the one-dimensional model. The percolation threshold in one-dimensional models is zero, i.e., even a single defect (jam in the present model) totally kills the conductivity (the running state). Which of the features of the model behavior will persist in a two-dimensional model is the subject for further investigations; some preliminary results are presented in Refs. [4,5].

ACKNOWLEDGMENTS

O.M.B. wishes to express his gratitude to Thierry Dauxois, Maxim Paliy, and Michel Peyrard for illuminating discussions. This work was supported in part by grants from the Hong Kong Research Grants Council (RGC) and Hong Kong Baptist University (FGR).

[1] B. N. J. Persson, Phys. Rev. Lett. **71**, 1212 (1993); Phys. Rev. B **48**, 18 140 (1993).
[2] F.-J. Elmer, Phys. Rev. E **50**, 4470 (1994); M. Weiss and F.-J. Elmer, Phys. Rev. B **53**, 7539 (1996).
[3] M. G. Rozman, M. Urbakh, and J. Klafter, Phys. Rev. Lett. **77**, 683 (1996); Phys. Rev. E **54**, 6485 (1996); Europhys. Lett. **39**, 183 (1997).
[4] O. M. Braun, T. Dauxois, M. V. Paliy, and M. Peyrard, Phys. Rev. Lett. **78**, 1295 (1997); Phys. Rev. E **55**, 3598 (1997).
[5] M. Paliy, O. Braun, T. Dauxois, and B. Hu, Phys. Rev. E **56**, 4025 (1997).
[6] O. M. Braun, A. R. Bishop, and J. Röder, Phys. Rev. Lett. **79**, 3692 (1997).
[7] O. M. Braun and Yu. S. Kivshar, Phys. Rev. B **50**, 13 388 (1994).
[8] H. Risken, *The Fokker-Planck Equation* (Springer, Berlin, 1984).
[9] C. W. Gardiner, *Handbook of Stochastic Methods* (Springer, Berlin, 1983).
[10] S. Katz, J. L. Lebowitz, and H. Spohn, J. Stat. Phys. **34**, 497 (1984).
[11] J. Krug, Phys. Rev. Lett. **67**, 1882 (1991).
[12] B. Derrida, E. Domany, and D. Mukamel, J. Stat. Phys. **69**, 667 (1992); B. Derrida, M. R. Evans, V. Hakim, and V. Pasquier, J. Phys. A **26**, 1493 (1993); G. Schütz and E. Domany, J. Stat. Phys. **72**, 277 (1993); M. R. Evans and B. Derrida, Acta Phys. Slov. **44**, 331 (1994).
[13] O. Braun and B. Hu, J. Stat. Phys. (to be published).
[14] L. D. Landau and E. M. Lifshitz, *Statistical Physics* (Pergamon, London, 1958).